ELECTRONIC RESEARCH ANNOUNCEMENTS
IN MATHEMATICAL SCIENCES
Volume 18, Pages 1–11 (January 25, 2011)
S 1935-9179 AIMS (2011)

doi:10.3934/era.2011.18.1

SPECIAL FUNCTIONS CREATED BY BOREL-LAPLACE TRANSFORM OF HÉNON MAP

CHIHIRO MATSUOKA AND KOICHI HIRAIDE

(Communicated by Boris Hasselblatt)

Abstract. We present a novel class of functions that can describe the stable and unstable manifolds of the Hénon map. We propose an algorithm to construct these functions by using the Borel-Laplace transform. Neither linearization nor perturbation is applied in the construction, and the obtained functions are exact solutions of the Hénon map. We also show that it is possible to depict the chaotic attractor of the map by using one of these functions without explicitly using the properties of the attractor.

1. Introduction

The Hénon map [1] is a model that exhibits the same property as the Lorenz system [2]. It was developed to describe the atmospheric turbulence on the basis of the Navier-Stokes equation. Since then, numerous researchers have used this map as the simplest model to describe the chaotic behavior in various dissipative systems. The strange attractor, which appears as the closure of the unstable manifold of the Hénon map, is often considered a model of unpredictable motion as it is well-known that the strange attractor's trajectory is nondeterministic. In this paper, we present an algorithm and a concrete functional form for describing the unstable manifold, as well as the stable manifold, of the Hénon map. We use the Borel-Laplace transform and asymptotic expansions to construct these functions. Hakkim and Mallick [3] calculated the separatrix splitting in a conservative system using the matched asymptotic expansions and Borel summation taking the standard map as an example. Tovbis *et al.* [4, 5] and Nakamura and Hamada [6] discussed the relation between the Borel-Laplace transform and the Stokes phenomenon using the Hénon map by selecting parameters for which the system becomes Hamiltonian, and calculated the splitting angle. The works [7, 8, 9] are based on the idea of *asymptotic expansions beyond all orders*, which is used to capture the exponentially small effects.

In addition to these singular perturbative approaches, there exist some alternative methods to compute exponentially small terms. Voros [10] proposed the *exact* WKB method to solve the quantum oscillator and Écalle [11, 12, 13] proposed the

Received by the editors June 8, 2010.
2000 *Mathematics Subject Classification.* Primary: 39A45; Secondary: 44A10.
Key words and phrases. Borel-Laplace transform, asymptotic expansion, difference equation, Hénon map.
This work is partially supported by a Grant-in-Aid for Scientific Research (C) from the Japan Society for the Promotion of Science.

resurgent analysis [14] to perform the resummation of divergent power series given by asymptotic expansions in differential equations. These methods enable us to calculate exponentially small terms without the perturbative approach. Gelfreich and Sauzin [15] applied the resurgent analysis to the Hénon map and calculated the splitting angle very accurately. An essential aspect of these works is that the systems considered can be reduced to a differential equation. In this paper, we consider the case of a system that cannot be reduced to a differential equation, i.e., a truly dissipative system. The purpose of our study is to construct special functions that can describe the stable and unstable manifolds in such systems and depict these manifolds with asymptotic expansions derived from the functions. We emphasize that no perturbative approaches, including linearizations, are used for the construction.

This paper is organized as follows. In Sec. 2, we recall the definition of the Borel-Laplace transform of the Hénon map. In Sec. 3, we present the special functions that describe the stable and unstable manifolds of the Hénon map. Using the asymptotic expansions of the functions described in Sec. 3, we depict the stable and unstable manifolds in Sec. 4.

2. Laplace transform of Hénon map

The Hénon map is a polynomial diffeomorphism $f : \mathbb{C}^2 \to \mathbb{C}^2$ defined by

$$f : \begin{pmatrix} x \\ y \end{pmatrix} \mapsto \begin{pmatrix} 1 + y - ax^2 \\ bx \end{pmatrix}, \tag{2.1}$$

where a and b are complex parameters [1]. The fixed points of this map are given as follows:

$$\left(\frac{b - 1 \pm \sqrt{(b-1)^2 + 4a}}{2a}, \quad \frac{b - 1 \pm \sqrt{(b-1)^2 + 4a}}{2a} b \right). \tag{2.2}$$

It is obvious that when a fixed point $P = (x_f, y_f)$ is a saddle point, the two eigenvalues, α_1 and α_2, of the derivative of f at P are the solutions of the quadratic equation $\alpha^2 + 2ax_f\alpha - b = 0$, where α_1 and α_2 satisfy $0 < |\alpha_1| < 1$ and $|\alpha_2| > 1$, respectively. We define the stable and unstable manifolds at the saddle point P by

$$W^s(P) \quad = \quad \{Q \in \mathbb{C}^2 | f^n(Q) \to P \text{ as } n \to \infty\}$$

and

$$W^u(P) \quad = \quad \{Q \in \mathbb{C}^2 | f^n(Q) \to P \text{ as } n \to -\infty\},$$

respectively. We will construct analytic functions that describe these manifolds by using the Borel-Laplace transform.

After shifting the fixed point P to the origin by $x \to x + x_f$ and $y \to y + y_f$, we introduce a parameter $t \in \mathbb{C}$ that parameterizes the stable and unstable manifolds via the equation $f\,[x(t), y(t)] = [x(t+1), y(t+1)]$. Then, the Hénon map (2.1) yields the following difference equation

$$x(t+1) - \lambda x(t) - bx(t-1) = -a\{x(t)\}^2, \tag{2.3}$$

where $\lambda = -2ax_f$, and $y(t)$ is given by $y(t) = bx(t-1)$. We remark that the boundary condition of $x(t)$ in (2.3) is determined by selecting one of the two saddle points present among the fixed points given in (2.2).

Now, we determine the solution of (2.3) in the form of a Laplace integral, given by

$$x(t) = \mathcal{L}[X](t) = \int_\gamma \mathrm{e}^{-\zeta t} X(\zeta)\mathrm{d}\zeta, \tag{2.4}$$

where the path γ depends on the position and form of singularities on X. Substituting (2.4) into (2.3), we obtain the following integral equation for the Borel transform, $X(\zeta)$, of $x(t)$:

$$AX = -aX * X + C \tag{2.5}$$

where $*$ denotes convolution defined by

$$F * G = \int_0^\zeta F(\zeta - \zeta')G(\zeta')\mathrm{d}\zeta',$$

A is defined by

$$A(\zeta) = \mathrm{e}^{-\zeta} - \lambda - b\mathrm{e}^{\zeta},$$

and C is a constant satisfying the relation $A(0)X(0) = C$. We assume that $X(\zeta)$ can be expanded as a Taylor series

$$X(\zeta) = a_0 + a_1\zeta + a_2\zeta^2 + \cdots \tag{2.6}$$

in a neighborhood of the origin, and we define $\tilde{X}$ by

$$X(\zeta) = a_0 + \tilde{X}(\zeta). \tag{2.7}$$

Substituting (2.6) and (2.7) into (2.5), we have

$$A\tilde{X} + 2aa_0 * \tilde{X} = W, \tag{2.8}$$

where

$$W = W_0 - a\tilde{X} * \tilde{X}$$

and

$$W_0 = -aa_0^2\zeta - a_0 A + C.$$

In order to develop an algorithm to determine the solution $\tilde{X}(\zeta)$, we formally expand $\tilde{X}(\zeta)$ and $W(\zeta)$ using a parameter σ as

$$\tilde{X}(\zeta) = \sum_{n=1}^{\infty} \sigma^n \tilde{X}_n(\zeta)$$

and

$$W(\zeta) = \sum_{n=0}^{\infty} \sigma^{n+1} W_n(\zeta).$$

We then substitute these expansions into (2.8). Then, we have

$$\begin{aligned} A\tilde{X}_1 + 2aa_0 * \tilde{X}_1 &= W_0, \\ A\tilde{X}_{n+1} + 2aa_0 * \tilde{X}_{n+1} &= -a\sum_{k=1}^{n} \tilde{X}_k * \tilde{X}_{n-k+1} = W_n \\ & \qquad (n = 1, 2, \dots), \end{aligned} \tag{2.9}$$

for each order of σ, where $\tilde{X}_n$ $(n = 1, 2, \cdots)$ is given as the solution to (2.8):

$$\tilde{X}_n = A^{-1}F_0 \int_0^\zeta \frac{W'_{n-1}}{F_0}\mathrm{d}\zeta', \quad F_0 = \left(\frac{\mathrm{e}^{-\zeta} - \alpha_1}{\mathrm{e}^{-\zeta} - \alpha_2}\right)^\beta, \tag{2.10}$$

where

$$\beta = 2aa_0/(\alpha_1 - \alpha_2).$$

In (2.10), the zeros of $A(\zeta)$, given by

$$\begin{aligned} \zeta_k^+ &= -\log|\alpha_1| + (2k\pi + \theta_+)i \\ \zeta_k^- &= -\log|\alpha_2| + (2k\pi + \theta_-)i \end{aligned} \tag{2.11}$$

for $k \in \mathbb{Z}$, are singularities of the function $\tilde{X}_n$, where $\theta_+ = \arg\alpha_1$ and $\theta_- = \arg\alpha_2$. We call these singularities, derived from the zeros of $A(\zeta)$, *first singularities*. The singularities ζ_k^+ and ζ_k^- coincide with each other and appear on the imaginary axis for $a = 1$ and $b = -1$ ($|\alpha_1| = |\alpha_2| = 1$, $\theta_+ = \theta_-$), i.e., the Hénon map is reduced to a Hamiltonian system [4, 5, 6, 15]. For the dissipative case, where in the Hénon attractor [1] appears, the parameters are assumed to be $a = 1.4$ and $b = 0.3$, for which $\theta_+ = 0$ and $\theta_- = \pm\pi$. When $|\alpha_1| < 1$ ($|\alpha_2| > 1$), i.e., for the stable (unstable) manifold, all singularities appear on the $\mathrm{Re}(\zeta) > 0$ ($\mathrm{Re}(\zeta) < 0$) plane. The two functions describing the stable and unstable manifolds are independent of each other. We remark that new singularities can be created by convolution when $\mathrm{Re}(\zeta_k^\pm) \neq 0$. After some lengthy calculations, we can prove that

$$a_0 = \frac{\alpha + b\alpha^{-1}}{2a},$$

where $\alpha = \alpha_1$ or α_2 ($\alpha \neq 0$) and $\beta = +1$ ($\beta = -1$) if $\alpha = \alpha_1$ ($\alpha = \alpha_2$). Given $a_0 = X(0)$, we can determine C in (2.5) as

$$C = \frac{(1 - \lambda - b)(\alpha + b\alpha^{-1})}{2a}$$

from the relation $C = A(0)X(0)$.

3. Borel transform of Hénon map

The algorithm for obtaining the solution $\tilde{X}$ is as follows. In order to simplify the discussion, we select a first singularity $\zeta_1 \equiv \zeta_0^\pm$. Taking into account that $\zeta = 0$ is a regular point of $\tilde{X}$, we perform the analytic continuation of $\tilde{X}$ starting from the origin. First, we expand A, F_0, and W_0 in (2.10) in a neighborhood of the origin and calculate the integral in $\tilde{X}_1$. In this calculation, ζ is bounded by ζ_1: $|\zeta| < \zeta_1$. Then, using this $\tilde{X}_1$, we calculate the convolution W_1 from the relation given by (2.9). Substituting W_1 into (2.10), we obtain $\tilde{X}_2$. Performing these calculations repeatedly, we obtain the solution up to $\tilde{X}_n$ ($n = 1, 2, \cdots$) in a neighborhood of the origin. Next, expanding A, F_0, and W_0 in a neighborhood of the first singularity ζ_1, we repeat the same calculations for $\tilde{X}_n$ and W_n ($n = 1, 2, \cdots$). The obtained $\tilde{X}$ can be continued analytically up to $|\zeta| < 2|\zeta_1|$. Further, we repeat these iterative calculations in neighborhoods of the higher-order singularities $\zeta = N\zeta_1$ ($N = 2, 3, \cdots$) derived from ζ_1. All singularities $N\zeta_1$ ($N \geq 2$) are created by convolution.

The iterative algorithm given by (2.9) and (2.10) yields the sequence

$$\tilde{X}_1 \mapsto W_1 \mapsto \tilde{X}_2 \mapsto W_2 \mapsto \ldots \mapsto W_{n-1} \mapsto \tilde{X}_n \mapsto \ldots.$$

We finally obtain the solution $\tilde{X}$ as follows:

Theorem 1. *Let $\zeta = N\zeta_1 + \xi$ $(N = 1, 2, \cdots)$ and the formal expanding parameter $\sigma = 1$. Then the solution $\tilde{X}(\zeta)$ of (2.8) is given as the limit of a Riemann surface $\tilde{X}^{(N)}(\zeta)$ as follows:*

$$\tilde{X}(\zeta) = \lim_{N\to\infty} \tilde{X}^{(N)}(\zeta), \quad \tilde{X}^{(N)}(\zeta) = \sum_{n=1}^{\infty} \tilde{X}_n^{(N)}(\zeta),$$

$$\tilde{X}_n^{(N)} = \begin{cases} \displaystyle\sum_{m=0}^{\infty} b_{n,m+n-1}^{(N)} \xi^{m+n-1} (\log \xi)^n + \mathrm{reg}^{(n-1)}(\xi), & (1 \le n \le N-1) \\ \displaystyle\sum_{m=0}^{\infty} b_{n,m+n-1}^{(N)} \xi^{m+n-1} (\log \xi)^N + \mathrm{reg}^{(N-1)}(\xi), & (n \ge N) \end{cases} \tag{3.1}$$

$$W_{n-1}^{(N)} = \begin{cases} \displaystyle\sum_{m=0}^{\infty} v_{n-1,m+n-1}^{(N)} \xi^{m+n-1} (\log \xi)^n + \mathrm{reg}^{(n-1)}(\xi), & (2 \le n \le N) \\ \displaystyle\sum_{m=0}^{\infty} v_{n-1,m+n-1}^{(N)} \xi^{m+n-1} (\log \xi)^N + \mathrm{reg}^{(N-1)}(\xi). & (n \ge N+1) \end{cases} \tag{3.2}$$

The notation $\mathrm{reg}^{(n-1)}$ $(n = 1, 2, \cdots)$ is defined by

$$\mathrm{reg}^{(n-1)}(\xi) = \sum_{m=0}^{n-1} R_m(\xi) (\log \xi)^m,$$

where $R_m(\xi) = * + *\xi + *\xi^2 + \cdots$ $(m = 0, 1, 2, \cdots)$ is a regular function with real coefficients $*$'s for real a and b.

If $a, b \in \mathbb{R}$, then the coefficients $b_{n,m+n-1}^{(N)}$ and $v_{n-1,m+n-1}^{(N)}$ are also real. Note that the form of the singularity at $N\zeta_1$ (the order of log) depends on the order of the convolution, n.

For the coefficients $b_{n,m+n-1}^{(N)}$ $(N = 1, 2, \cdots)$ in (3.1) the following result holds.

Theorem 2. *The coefficients $b_{n,m+n-1}^{(N)}$ $(N = 1, 2, \cdots)$ in (3.1) are given by*

$$b_{n,m+n-1}^{(1)} = \sum_{m=0}^{l} \sum_{m'=0}^{m} c_{l-m}^{(1)} f_{m-m'-1}^{(1)} v_{n-1,n-1+k+m'}^{(1)} \frac{n+m'+k-1}{n+m+k-2}, \quad (n \ge 1) \tag{3.3}$$

where

$$v_{n-1,n-1+l+k}^{(1)} = -2a \sum_{m=0}^{l} a_{k,2k-1+l-m} b_{n-k,n-k-1+m}^{(1)} \sum_{r=0}^{2k-1+l-m} {}_{2k-1+l-m}C_r \frac{(-1)^r}{n-k+m+r} \quad (k \ge 1,\ n \ge 2)$$

when $N = 1$.

When $N \geq 2$, the coefficient $b^{(N)}_{n,n-1+l}$ has the following form:

$$b^{(N)}_{n,n-1+l} = \sum_{k=0}^{l}\sum_{l'=0}^{l-k} c^{(N)}_{l'} f^{(N)}_{l-k-l'} v^{(N)}_{n-1,n-1+k} \frac{k+n-1}{n-1+l-l'}, \quad (n \geq N) \tag{3.4}$$

in which

$$\begin{aligned}
\tilde{v}^{(N)}_{n-1,l+n-1} &= \sum_{L=1}^{N-1}\sum_{k'=N-L}^{n-L}\sum_{m'=0}^{l} b^{(N-L)}_{k',k'-1+m'} b^{(L)}_{n-k',n-k'-1+l-m'} \\
&\quad \times \sum_{r=0}^{k'-1+m'} {}_{k'-1+m'}C_r \frac{(-1)^r \left(\frac{L}{N}\right)^{n-k'+l-m'+r}}{n-k'+l-m'+r}, \\
\hat{v}^{(N)}_{n-1,n-1+l} &= \sum_{k"=1}^{n-N}\sum_{m"=0}^{l-k"} a_{k",2k"-1+m"} b^{(N)}_{n-k",n-2k"-1+l-m"} \\
&\quad \times \sum_{r'=0}^{2k"-1+m"} {}_{2k"-1+m"}C_{r'} \frac{(-1)^{r'}}{n-2k"+l-m"+r'}, \\
v^{(N)}_{n-1,l+n-1} &= -2a\left(\tilde{v}^{(N)}_{n-1,l+n-1} + \hat{v}^{(N)}_{n-1,n-1+l}\right).
\end{aligned}$$

After some tedious calculations, we can estimate the coefficient $b^{(N)}_{n,m+n-1}$ $(m = 0, 1, 2, \cdots)$ in the solution $\tilde{X}^{(N)}_n(\zeta_N + \xi)$ $(n \geq N)$ as follows.

Theorem 3. *There exist constants $K_N > 0$ and $L_N > 0$ ($|K_N| < 1$ and $|L_N| < 1$) depending on a, b, and N such that*

$$\begin{aligned}
|b^{(N)}_{n,n-1}| &\leq \frac{K_N^n |\alpha_1|^{N\log N}}{n!}, \\
|b^{(N)}_{n,m+n-1}| &\leq L_N^m |b^{(N)}_{n,n-1}|,
\end{aligned} \tag{3.5}$$

for all $n \geq N$ $(N \geq 1)$. When one considers the unstable manifold, α_1 in (3.5) is replaced with $(\alpha_2)^{-1}$.

In order to perform the Laplace transform of $X(\zeta) = a_0 + \tilde{X}(\zeta)$, we have to uniformize the multivalued function X and construct a univalued function. We do not discuss the uniformization method in detail here. The resulting Laplace transform $x(t)$ is given by the following theorem.

Theorem 4. *The solution to the difference equation (2.3) is uniquely determined as follows:*

$$\begin{aligned}
x(t) &= \int_\gamma \mathrm{e}^{-\zeta t} X(\zeta) \mathrm{d}\zeta \\
&= \lim_{N\to\infty} \frac{1}{(2\pi i)^{\frac{N(N+1)}{2}}} \int_{-\infty \mathrm{e}^{i\theta}}^{\infty \mathrm{e}^{i\theta}} \mathrm{e}^{-\zeta t} X_R(\zeta, N) \mathrm{d}\zeta,
\end{aligned} \tag{3.6}$$

where

$$X_R(\zeta, N) = (2\pi i)^{\frac{N(N+1)}{2}} \sum_{m=0}^{\infty} b^{(N)}_{N,m+N-1} \xi^{m+N-1} \tag{3.7}$$

and $X_R(\zeta, N)$ is the uniformized function of $X(\zeta)$, which depends on the N-th singularity $N\zeta_1$. The argument θ in the integral (3.6) is the angle connecting the origin and $N\zeta_1$.

The Laplace transformed function $x(t)$ in (3.6) is an entire function, i.e., this function does not have singularities on the t-plane, except at infinity. We emphasize that the Laplace transform (3.6) is performed over $(-\infty, \infty)$, and not $[0, \pm\infty)$. The estimate (3.5) guarantees the existence of this infinite integral, i.e., due to the existence of the term $|\alpha_1|^{N \log N}$ ($|\alpha_1| < 1$) in (3.5), the exponential growth at $t = -\infty$ when $\mathrm{Re}(\zeta) > 0$ ($t = \infty$ when $\mathrm{Re}(\zeta) < 0$) is suppressed by taking $N \to \infty$. This fact enables us to depict the stable and unstable manifolds with the asymptotic expansion; as shown in the next section.

4. Asymptotic expansions and stable and unstable manifolds

In this section, we describe the stable and unstable manifolds of the Hénon map by using the asymptotic expansion of $x(t)$, as given in (3.6). The asymptotic expansion of $x(t)$ is provided by the following theorem.

Theorem 5. *The asymptotic expansion of $x(t)$, as given in (3.6), has the form*

$$\begin{aligned} x(t) &\sim \sum_{N=1}^{\infty} \mathrm{e}^{\pm N\zeta_1 t} \sum_{m=N-1}^{\infty} \frac{b_{N,m}^{(N)} m!}{(\pm t)^{m+1}} \\ &= \sum_{N=1}^{\infty} \mathrm{e}^{\pm N\zeta_1 t} \frac{b_{N,N-1}^{(N)} (N-1)!}{(\pm t)^N} \left(1 + O(|t|^{-1})\right), \end{aligned} \tag{4.1}$$

where the $+$ and $-$ signs correspond to the stable and unstable manifolds, respectively.

Due to the estimate (3.5), the asymptotic expansion (4.1) converges for all $t \in \mathbb{C}$ except for the origin $t = 0$; therefore, this expansion is not formal. To depict the stable and unstable manifolds, we apply the following property of the dynamical system:

$$\begin{aligned} f^{\mp n}[x(t)] &= x(t \mp n) \\ &\sim \sum_{N=1}^{\infty} \mathrm{e}^{-N\zeta_1 (t \mp n)} \frac{b_{N,N-1}^{(N)} (N-1)!}{(\pm t)^N}, \end{aligned} \tag{4.2}$$

where the upper (lower) sign in $\mp$ (or $\pm$) corresponds to the stable (unstable) manifold and n is a large positive integer. When $\mathrm{Re}(t) > 0$ and $\mathrm{Re}(t) - n < 0$, the curve $(x, y) = [x(t-n), bx(t-n-1)]$ describes the stable manifold. However, when $\mathrm{Re}(t) > 0$ and $\mathrm{Re}(t) - n > 0$, the curve $[x(t-n), bx(t-n-1)]$ tends to the fixed point P due to the relation $\lim_{n\to\infty} f^n[x(t)] \to P$. When $\mathrm{Re}(t) < 0$ and $\mathrm{Re}(t) + n > 0$, the curve $(x, y) = [x(t+n), bx(t+n-1)]$ describes the unstable manifold. On the other hand, when $\mathrm{Re}(t) < 0$ and $\mathrm{Re}(t) + n < 0$, the curve $[x(t+n), bx(t+n-1)]$ tends to the fixed point P since $\lim_{n\to-\infty} f^n[x(t)] \to P$. We remark that the asymptotic expansion given by (4.2) is not the one obtained by the shift $t \to t \mp n$ in the expansion of $x(t)$ in (4.1).

Figures 1 and 2 show the stable and unstable manifolds obtained by using the asymptotic expansion (4.2). Here, $\zeta_1 = -\log|\alpha_1|$ and $\zeta_1 = -\log|\alpha_2| - \pi i$ for

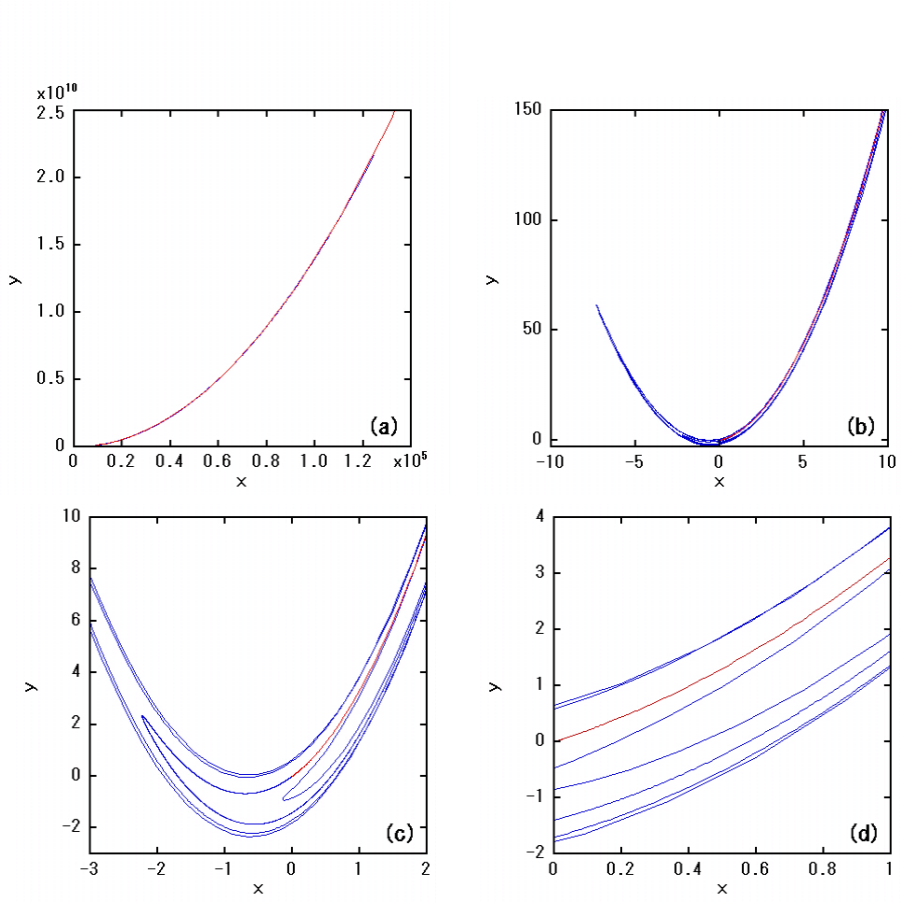

FIG. 1. Stable manifold of the Hénon map described by the asymptotic expansion given in (4.2) for the parameters $a = 1.4$ and $b = 0.3$. The fixed point is shifted to the origin. (a) depicts the wide view of the stable manifold and (b) is an enlarged view of (a). (c) is an enlarged view of (b), and (d) is an enlarged view of (c). The regions (a) $-10 \le x \le 1.4 \times 10^5$ and $-3 \le y \le 2.5 \times 10^{10}$, (b) $-10 \le x \le 10$ and $-3 \le y \le 150$, (c) $-3 \le x \le 2$ and $-3 \le y \le 10$, and (d) $0 \le x \le 1$ and $-2 \le y \le 4$ are drawn.

the stable and unstable manifolds, respectively. We have $-\log|\alpha_1| \sim 1.858$ and $-\log|\alpha_2| \sim -0.654$ for $a = 1.4$ and $b = 0.3$.

These values suggest that $x(t-n)$ in (4.2) (stable manifold) is real when t is real, while $x(t+n)$ (unstable manifold) is complex when t is real. Regarding the argument θ in the Laplace transform (3.6), $\theta = 0$ for the stable case and $\theta = \tan^{-1}(-\pi/\log|\alpha_2|)$ for the unstable case. The coefficient $b^{(N)}_{N,N-1}$ in (4.2) is obtained by solving (3.3) and (3.4) iteratively. In order to avoid the effects of the roundoff error, the calculations for $b^{(N)}_{N,N-1}$ are performed with 128 digits of precision

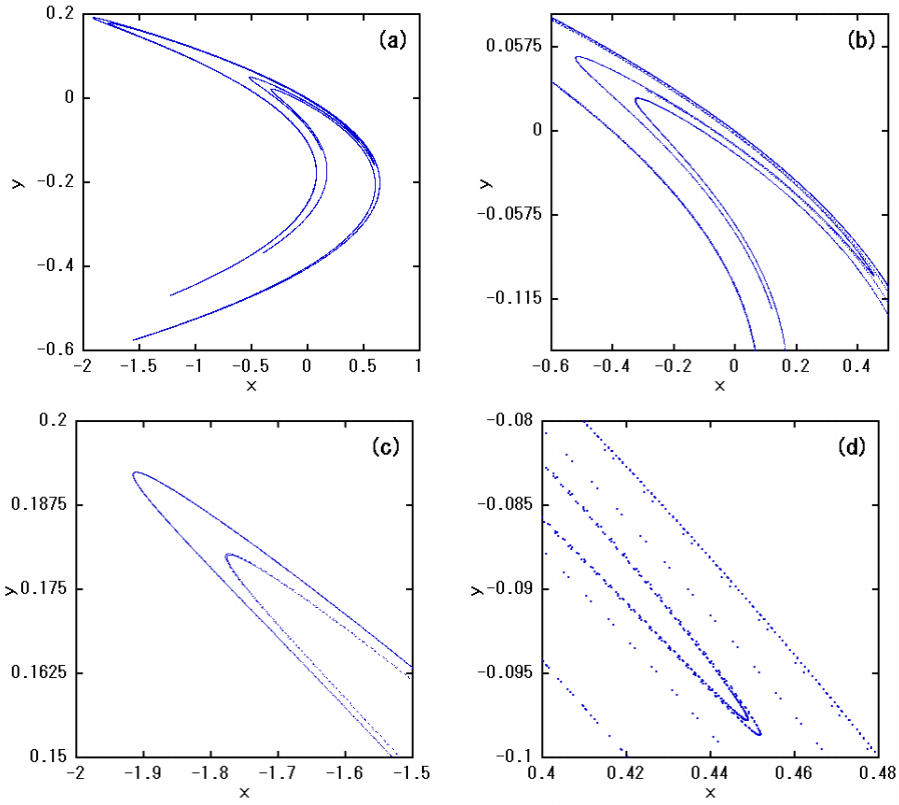

FIG. 2. Unstable manifold of the Hénon map described by the the asymptotic expansion given in (4.2) where the parameters are identical to Fig. 1 and the fixed point is shifted to the origin. (a) depicts the entirety of the unstable manifold, (b) and (c) are enlarged views of (a), and (d) is an enlarged view of (b). The depicted regions are (a) $-2 \leq x \leq 1$ and $-0.6 \leq y \leq 0.2$, (b) $-0.6 \leq x \leq 0.5$ and $-0.15 \leq y \leq 0.08$, (c) $-2 \leq x \leq -1.5$ and $0.15 \leq y \leq 0.2$, and (d) $0.4 \leq x \leq 0.48$ and $-0.1 \leq y \leq -0.08$.

for both the stable and unstable cases. For this particular demonstration, we have selected the parameters $N = 200$ and $n = 20000$.

In Fig. 1, we can take the parameter t to be real. The blue and red solid lines depict the region $19990.5 \leq t \leq 20000$ in $(x, y) = [x(t-n), bx(t-n-1)]$ and $-20010 \leq t \leq -20000$ in $(x, y) = [x(t+n), bx(t+n+1)]$, respectively. The latter cannot be depicted continuously from the former when t is real. For the blue and red lines, 40000 and 5000 plot points, respectively, are considered. We remark that $(x, y) = [x(t-n), bx(t-n-1)]$ ($(x, y) = [x(t+n), bx(t+n+1)]$) is continuous with respect to real t (see the discussion for the unstable case below). The blue and red lines in the first quadrant in Fig. 1 (a) extend up to the order of $(x, y) \sim (10^5, 10^{10})$, while the (blue) line in the second quadrant extends to approximately $(x, y) \sim (-7.34, 61.8)$. The oscillatory motion exhibited by the blue

line spans these two regions.The value of y in the first quadrant increases with $-(t-n)$, and hence, tends to infinity as $t-n \to -\infty$. The red line in the first quadrant is expected to tend to infinity without the oscillation.

For the unstable case, $x(t+n)$ is not real-valued when t is real. Therefore, in order to depict the unstable manifold, we cut the manifold $(x, y) = [x(t+n), bx(t+n-1)]$ at points for which the imaginary part of (x, y) becomes zero and project the resulting section onto $\mathbb{R}^2$. The algorithm for calculating the points for which $\mathrm{Im}(x, y) = 0$ is as follows. We first note that from the asymptotic expansion (4.2), we can easily see $\mathrm{Im}(x) = 0$ when t is integer. Taking this into account, we first divide the complex t-plane into rectangles such that an integer is set to one of the vertices. Then, we identify the points t such that the distance from the real axis satisfies the condition $s(t) \equiv \sqrt{x_i(t)^2 + y_i(t)^2} = 0$, starting from the neighborhood of one integer to the next integer in turn, where $x_i(t) = \mathrm{Im}[x(t+n)]$ and $y_i(t) = \mathrm{Im}[bx(t+n-1)]$. One integer is divided further into fine grid points. We divide one integer into 10^6 parts, i.e., there exist 10^6 grid points between one integer and the next integer in the real t direction. We also set 10^6 grid points between two adjacent integers in the positive imaginary t direction.

Figure 2 shows the unstable manifold obtained by substituting the points t satisfying $s(t) = 0$ into $[x(t+n), bx(t+n-1)]$. In this example, the only points t that satisfy $s(t) = 0$ within the precision are integers, and the other points are selected such that $s(t)$ takes minimum values within a rectangle having integers as vertices. The minimum points t_m $(m = 1, 2, \cdots)$ obtained with this method are periodic and are given by $t_m = m(\triangle t_r + i\triangle t_i)$, where $\triangle t_r = 2.5 \times 10^{-5}$ and $\triangle t_i = 1.2 \times 10^{-4}$. That is, the minimum points appear on the line with slope $\triangle t_i / \triangle t_r = 4.8$.

For Fig. 2 (a), the integers that satisfy $-20000 \le \mathrm{Re}(t) \le -19980$ are taken. We set $t(\in \mathbb{C})$ as $t = t_r + it_i$, and detect the points which satisfy $|s(t)| \le 10^{-5}$ (we call these minimum points) over the region $-20000 \le t_r \le -19980$ and $0 \le t_i \le 1$. In order to carry out this detection, one integer is divided into 10^6 grid points, i.e., the above rectangular region ($-20000 \le t_r \le -19980$ and $0 \le t_i \le 1$) is composed of $20 \times 10^6 \times 10^6$ grid points. The number of points detected exceeds 10^5, and all of these points form the unstable manifold. If we adopt all these points to depict the unstable manifold, the points are too 'dense' and the fine structure in the unstable manifold 'collapses'. Therefore, we 'thin' these minimum points to 21407 (see below), following the rule described in the next paragraph. Mathematically, these manipulations including the method in next paragraph are nonessential. When we depict the points $(\mathrm{Re}(x), \mathrm{Re}(y))$ satisfying such $s(t)$, Fig. 2 is obtained.

For integers with $0 \le |\mathrm{Re}(t) + n| \le 10$, we select $m = 100$ in t_m, while we select $m = 10$ and $m = 1$ when $11 \le |\mathrm{Re}(t) + n| \le 16$ and $17 \le |\mathrm{Re}(t) + n| \le 20$, respectively. Due to the round-off error, the minimum points t_m are difficult to compute as $|\mathrm{Re}(t)+n|$ increases and t approaches the next integer within an interval. Figure 2 (a) is generated with 21407 points. The unstable manifold cannot be visualized by interpolating the points.

The solutions of the Hénon map $x(t)$ are independent when a path in the Laplace transform is fixed and there exist countable infinite paths for one set of (a, b). Once the unstable manifold is described using the function, we can calculate the entropy in the system from the length of the curves in the unstable manifold [16]. Therefore,

the function that we obtained here can be used to study the thermodynamics of dissipative systems.

References

[1] M. Hénon, *A two-dimensional mapping with a strange attractor*, Commun. Math. Phys., **50** (1976), 69–77. MR 0422932

[2] E. N. Lorenz, *Deterministic nonperiodic flow*, J. Atmos. Sci., **20** (1963), 130–141.

[3] V. Hakim and K. Mallick, *Exponentially small splitting of separatrices, matching in the complex plane and Borel summation*, Nonlinearity, **6** (1993), 57–70. MR 1203052

[4] A. Tovbis, *Asymptotics beyond all orders and analytic properties of inverse Laplace trnsforms of solutions*, Commun. Math. Phys., **163** (1994), 245–255. MR 1284784

[5] A. Tobvis, M. Tsuchiya and C. Jaffe, *Exponential asymptotic expansions and approximations of the unstable and stable manifolds of singularly perturbed systems with the Hénon map as an example*, Chaos, **8** (1998), 665–681. MR 1645522

[6] K. Nakamura and M. Hamada, *Asymptotic expansion of homoclinic structures in a symplectic mapping*, J. Phys. A, **29** (1996), 7315–7327. MR 1421940

[7] V. F. Lazutkin, I. G. Schachmannski and M. B. Tabanov, *Splitting of separatrices for standard and semistandard mappings*, Physica D, **40** (1989), 235–248. MR 1029465

[8] M. D. Kruskal and H. Segur, *Asymptotics beyond all orders in a model of crystal growth*, Stud. Appl. math., **85** (1991), 129–181. MR 1115186

[9] H. Segur, S. Tanveer and H. Levine (eds), "Asymptotics Beyond All Orders," (Plenum, New York), 1991.

[10] A. Voros, *The return of quartic oscillator: The complex WKB method*, Ann. Inst. H. Poincaré **39** (1983), 211–338. MR 0729194

[11] J. Écalle, "Les Fonctions Résurgence vol. 1," (French) [Resurgent functions. Vol. I] Les algèbres de fonctions résurgentes. [The algebras of resurgent functions] With an English foreword. Publications Mathématiques d'Orsay 81 [Mathematical Publications of Orsay 81], 5. Université de Paris-Sud, Département de Mathématique, Orsay, 1981. MR 0670417

[12] J. Écalle, "Les Fonctions Résurgence vol. 2," (French) [Resurgent functions. Vol. II] Les fonctions résurgentes appliquées à l'itération. [Resurgent functions applied to iteration] Publications Mathématiques d'Orsay 81 [Mathematical Publications of Orsay 81], 6. Université de Paris-Sud, Département de Mathématique, Orsay, 1981. MR 0670418

[13] J. Écalle, "Les Fonctions Résurgence vol. 3," (French) [Resurgent functions. Vol. III] L'équation du pont et la classification analytique des objects locaux. [The bridge equation and analytic classification of local objects] Publications Mathématiques d'Orsay [Mathematical Publications of Orsay], 85-5. Université de Paris-Sud, Département de Mathématiques, Orsay, 1985. MR 0852210

[14] B. Y. Sternin and V. E. Shatalov, "Borel-Laplace Transform and Asymptotic Theory," Introduction to Resurgent Analysis, CRC Press, Boca Raton, FL, 1996.

[15] V. Gelfreich and D. Sauzin, *Borel summation and splitting of separatrices for the Hénon map*, Ann. Inst. Fourier (Grenoble), **51** (2001), 513–67. MR 1824963

[16] S. Newhouse and T. Pignataro, *On the estimation of topological entropy*, J. Stat. Phys., **72** (1993), 1331–1351. MR 1241542

Department of Physics, Graduate school of Science and Technology, Ehime University, Bunkyocho 2-5, Matsuyama 790-8577, Japan

E-mail address: matsuoka@phys.sci.ehime-u.ac.jp

Department of Mathematics, Graduate school of Science and Technology, Ehime University, Bunkyocho 2-5, Matsuyama 790-8577, Japan

E-mail address: hiraide@ehimegw.dpc.ehime-u.ac.jp